Development and validation of an LC-FTMS method for quantifying natural sweeteners in wine

Syntia Fayad, Blandine Cretin and Axel Marchal*

Univ. de Bordeaux, ISVV, EA 5477, Unité de recherche ŒNOLOGIE, USC 1366 INRA, F-33882 Villenave d'Ornon, France

* Corresponding author: Axel Marchal, Univ de Bordeaux, ISVV, EA 4577, Unité de recherche ŒNOLOGIE, F-33882 Villenave d'Ornon, France.

e-mail: axel.marchal@u-bordeaux.fr; Tel: +33 557575867; Fax: +33 557575813

Abstract

The quality of a wine largely depends on the balance between its sourness, bitterness and sweetness. Recently, *epi*-dihydrophaseic acid-3′-*O*-*β*-glucopyranoside (*epi*-DPA-G) and astilbin, two molecules obtained from grapes, have been shown to contribute notably to the sweet taste of dry wines. To study the parameters likely to affect their concentration, a new method was developed and optimized by LC-FTMS. Three gradients and five C18 columns were tested. Good results in terms of linearity ($r^2 > 0.9980$), repeatability (RSD ≤ 3%), recovery (≥ 89 %) and LOQ (≤ 20 µg.L^{-1}) were obtained. The method was used to screen *epi*-DPA-G and astilbin in red wines of several vintages over one century. Both compounds were detected in all wines at concentrations varying from 1.2 to 14.7 mg/L for *epi*-DPA-G and from 0.5 to 42.6 mg/L for astilbin. Therefore, this new method can be used to quantify *epi*-DPA-G and astilbin reliably in wine.

Keywords: Orbitrap, method validation, wine, *epi*-DPA-G, astilbin, sweetness

1. Introduction

Wine is an alcoholic beverage that has been produced and praised for thousands of years on almost every continent and is considered to be a combination of art and science (Haseeb, Santi, Liprandi, & Baranchuk, 2019). At the molecular level, it consists of a matrix containing thousands of different molecules in several compound classes, all suspended in a hydro-ethanolic medium at varying concentrations (De Revel et al., 2017; Lorrain, Ky, Pechamat, & Teissedre, 2013; Markoski, Garavaglia, Oliveira, Olivaes, & Marcadenti, 2016). These compounds can be extracted from grapes, synthesized by microorganisms, released from oak wood during winemaking, and even formed during bottle aging (Ribereau-Gayon, Dubourdieu, Doneche, & Lonvaud, 2017). Therefore, the taste, aroma and composition of wine can be understood by studying grapes and wine chemistry. Scientific breakthroughs in enology have led to practical benefits and have significantly contributed to better monitoring of winemaking.

The sensory properties of a wine are major elements that determine its success among consumers and thus its value (Coste, Sousa, & Malfeito-Ferreira, 2018; Francis & Williamson, 2015; Loureiro, Brasil, & Malfeito-Ferreira, 2016). For example, consumers' spontaneous appetite for the sweet taste in wine is well known (MadalenaSena-Esteves, Mota, & Malfeito-Ferreira, 2018). Wine sweetness is important because it contributes to the gustatory balance by reducing the acidity, bitterness and astringency generated by organic acids and polyphenols (Hufnagel & Hofmann, 2008). These sensory interactions occur even in dry wines, i.e. wines with sugar contents far lower than their detection threshold. In dry wines, it has been shown that sweetness increases with the contact of yeast lees (Marchal, Marullo, Moine, & Dubourdieu, 2011) and during oak aging (Marchal, Pons, Lavigne, & Dubourdieu, 2013). These phenomena have been explained at the molecular level by demonstrating respectively the contribution of the protein

Hsp12 (Marchal, Marullo, et al., 2011) and by identifying sweet oak triterpenoids called quercotriterpenosides (QTT) (Marchal, Waffo-Teguo, Génin, Mérillon, & Dubourdieu, 2011).

Recently, several sweet-tasting compounds from grapes, and especially seeds, have been identified in dry wines (Crétin, Waffo-Teguo, Dubourdieu, & Marchal, 2019, p.), especially *epi*-dihydrophaseic acid-3'-*O*-β-glucopyranoside, *epi*-DPA-G and astilbin (Crétin, 2016; Crétin et al., 2019). Astilbin is a flavonoid, while *epi*-DPA-G is a glucosylated abscisic acid derivate (Del Refugio Ramos et al., 2004). The identification of these compounds in wine has opened promising perspectives to better understand the molecular determinism of wine taste and to monitor its balance. For this reason, a reliable quantitation method is needed to establish the influence of viticultural and enological factors on *epi*-DPA-G and astilbin concentrations in wine.

As wine is a complex matrix containing thousands of compounds and because some of them can have a significant sensory impact even at trace level, elucidating the molecular determinants of wine taste requires overcoming a dual challenge (L. Waterhouse, L. Sacks, & W. Jefferey, 2016). First, the use of analytical assays must allow the resolutive separation of wine components. For instance, high performance liquid chromatography (HPLC), gas chromatography (GC) and/or capillary electrophoresis (CE) have already been used (Acunha, Simó, Ibáñez, Gallardo, & Cifuentes, 2016; V. Esteves, Lima, Lima, & Duarte, 2004; Malec et al., 2017; Pinto et al., 2019). Sensitive and selective spectroscopic techniques such as mass spectrometry (MS) or nuclear magnetic resonance must be used to identify active compounds (Pinto et al., 2019).

In particular, liquid chromatography (LC) coupled to Fourier transform mass spectrometry (FTMS) with an Orbitrap analyzer has been used for a decade to analyze a broad range of compounds in various foods and beverages. The method is very sensitive and covers a wide dynamic range (Hogenboom, van Leerdam, & de Voogt, 2009). In combination with a high mass

resolution and accuracy in mass measurement, it is particularly powerful for applications involving structural identification, qualitative screening and quantification.

In this work, a new LC-FTMS method was developed to quantify *epi*-DPA-G and astilbin in wine. Three different gradients were tested on five different C18 columns, and performance parameters such as linearity, inter- and intra-day repeatability of retention time and peak area (RSD_{tr} and RSD_A), sensitivity (LOD, LOQ) and recovery were evaluated. The validated method was successfully applied to quantify these sweet molecules in several commercial wines. Sixteen vintages of a famous Burgundy estate were analyzed to assess the presence of the two sweet-tasting compounds in old wines up to one century old. These results established the first quantitative data of *epi*-DPA-G in wine.

2. Materials and methods

2.1. Chemicals and commercial wines

Ultrapure water (Milli-Q purification system, Millipore, France) and HPLC grade methanol (VWR International, Pessac, France) were used for sample preparation. Acetonitrile, water LC-MS grade and formic acid used for mass spectrometry analysis were purchased from Fisher Chemical (Illkirch, France). Sixty-eight commercial red wines from 1918 to 2017 obtained from different varieties and areas were analyzed to assess the presence of astilbin and *epi*-DPA-G (**Table 1**).

2.2. Sample preparation

Stock solutions of *epi*-DPA-G and astilbin (chromatographically pure at 96 %), isolated in a previous study (Crétin et al., 2019) were prepared in methanol at 1 mg/mL and stored at 4 °C.

Each sample of commercial wine was diluted to 1/3 in pure water and 0.45 µm-filtered before injection in LC-FTMS in order to prevent column saturation and to decrease the ethanol level likely to affect the chromatographic separation.

2.3. Instrumentation and operating conditions

The LC-FTMS platform consisted of an HTC PAL autosampler (CTC Analytics AG, Zwingen, Switzerland), an Accela U-HPLC system with quaternary pumps and an Exactive Orbitrap mass spectrometer equipped with a heated electrospray ionization (HESI I) probe (both from Thermo Fisher Scientific, Les Ulis, France). Different C18 columns were tested in this study: Hypersil Gold (2.1 mm x 100 mm, 1.9 µm), Syncronis™ (100 mm x 2.1 mm, 1.7 µm) from Thermo Fisher Scientific, High Silica Strength (HSST3; 100 mm x 2.1 mm, 1.8 µm), Bridged Ethylsiloxane/silica Hybrid (BEH; 100 mm x 2.1 mm, 1.7 µm) from Waters and Kinetex (100 mm x 2.1 mm, 1.7 µm) from Phenomenex. All the columns were protected by a guard column. Five µL of each sample were injected in a full injection mode. When using HSST3, BEH and Syncronis, the gradient ran at a constant flow rate of 400 µL/min while with Hypersil and Kinetex the flow rate was set at 600 µL/min. The eluents were (A) 0.1 % formic acid in water and (B) 0.1 % formic acid in acetonitrile. Three different gradients were tested. Gradient **I** consisted of 5 % (B) at 0 min; 5 % at 1 min; 30 % at 5.30 min; 98 % at 6.20 min ; 98 % at 6.45 min ; 5 % at 7.80 min and 5 % at 9 min. Gradient **II** consisted of 2 % (B) at 0 min; 2 % at 1 min; 25 % at 5 min; 98 % at 5.30 min ; 98 % at 6.30 min ; 2 % at 6.45 min and 2 % at 9 min. Gradient **III** consisted of 10 % (B) at 0 min; 15 % at 1 min; 25 % at 3 min; 80 % at 5.5 min; 90 % at 7.5 min and 10 % at 9 and 10 min.

Mass acquisitions were performed in negative Fourier Transform Mass Spectrometry (FTMS) ionization mode at a resolution of 10 000 (m/Δm, fwhm at 200 Th). The mass analyzer was

132 calibrated each week using Pierce® ESI Negative Ion Calibration Solution (Thermo Fisher
133 Scientific). The sheath and auxiliary gas flows (both nitrogen) were optimized at 80 and 15
134 arbitrary units, respectively. The HESI probe and capillary temperatures were 320 and 350 °C,
135 respectively. The electrospray voltage was set at – 3.5 kV, the capillary voltage to – 25 V, the
136 tube lens voltage offset to – 120 V and the skimmer voltage to – 20 V. Mass spectra were
137 recorded from 160 to 2000 Th, with an AGC value of 10^6. All data were processed using the
138 Qualbrowser and Quanbrowser applications of Xcalibur version 2.1 (Thermo Fischer Scientific).

139 ### *2.4. Method validation*

140 To choose the best chromatographic conditions and to validate the LC-FTMS method, the
141 following parameters were evaluated on the five columns in a PO1988.

142 #### *2.4.1. Calibration curve and linearity*

143 Calibration curves were designed by plotting the *epi*-DPA-G and astilbin areas obtained (*yi*)
144 against the nominal concentration of each calibration standard (*xi*). Different concentrations were
145 tested; 0.02, 0.05, 0.08, 0.2, 0.5, 0.8, 1, 5, 8 and 10 mg/L. Linear regression was performed and
146 the correlation coefficient (r^2), slope (a) and intercept (b) were determined.

147 #### *2.4.2. Intra- and inter-day precision (RSD)*

148 Intra- and inter-assay accuracy and precision were evaluated for *epi*-DPA-G and astilbin by terms
149 of relative standard deviation (RSD) on retention time (tr) and peak area (A) with five replicates
150 (n=5) at seven different levels on a single assay and five assays on three non-consecutive days.

151 #### *2.4.3. Limits of detection (LOD) and quantification (LOQ)*

Due to high mass accuracy, the noise level in the Orbitrap mass spectrometer, especially at *m/z* > 200, is virtually absent. Consequently, a standard signal-to-noise approach to determine LOQ and LOD is not relevant (De Paepe et al., 2013). Therefore, LOD and LOQ were estimated using an approach of linearity recommended by the International Organization of Vine and Wine (www.oiv.int/public/medias/2754/oiv-ma-as1-12fr.pdf). It uses the data obtained from the linearity or calibration curve such as the slope *a* and the standard deviation of the intercept of the regression *Sb*. Therefore, Sb corresponds to:

$$Sb = Sres \sqrt{\left(\frac{1}{np} + \frac{Mx^2}{\sum p(xi - Mx^2)}\right)} \quad \textbf{(1)}$$

And Sres to:

$$Sres = \sqrt{\frac{\sum_{i=1}^{n}\sum_{j=1}^{p}(yi,j - \ddot{y}i,j)^2}{pn-2}} \quad \textbf{(2)}$$

Where n=number of injections; p= number of repetitions;

Mx^2= average of x values and ÿj= theoretical value obtained from the calibration curve

Using these parameters, LOD corresponds to (3 x Sb)/a and LOQ to (10 x Sb)/a.

2.5. Study of commercial wines

The appropriate chromatographic conditions were used to screen and quantify the *epi*-DPA-G and astilbin present in different vintages of red wine (**Table 1**).

2.6. Recovery

Recovery was analyzed with three different samples of wines (PO1999b, SES2001 and VPCR1992) spiked with three concentrations of *epi*-DPA-G and astilbin (100 µg/L, 500 µg/L and 1 mg/L; n=3). The concentration determined by means of the calibration model was

compared to the real concentration of the standard by calculating the recovery rate ((determined concentration/real concentration) × 100) (Thompson, Ellison, & Wood, 2002).

3. Results and discussion

3.1. Optimization of chromatographic conditions

A taste-guided methodology was previously developed to isolate sweet compounds from wine. Their chemical structure was determined by HRMS and NMR (Crétin et al., 2019). This latter study has led to significant advances in knowledge of wine flavor by revealing sweet compounds obtained from grapes, especially *epi*-DPA-G and astilbin. In addition, a method for quantitating their presence and concentrations in various commercial wines was developed in the present work. Given the chemical complexity of the wine matrix, it was appropriate to use LC-FTMS.

Previously, Huang and Liaw (Huang & Liaw, 2017) developed a UPLC-DAD-MS method to analyze astilbin in *Hypericum formosanum* using the XBridge C18 column and a mobile phase composed of 0.1 % formic acid in water and (B) 0.1 % formic acid in acetonitrile. They demonstrated that flavonoids such as astilbin exhibit stronger signal responses in negative ion mode than positive ion mode. Therefore, the negative ion mode was used in this study. First, the chromatographic conditions of this method were optimized. Given the logP values of astilbin and *epi*-DPA-G (1.09 and -1.27 respectively), the retention time of astilbin on the C18 column was expected to be higher than that of *epi*-DPA-G. The values were estimated using Chemaxon software (ChemAxon Kft., Budapest, Hungary) at https://www.chemaxon.com/marvin/sketch/. Acetonitrile was used as the organic part of the mobile phase because it is more suitable for faster elution of the low polarity polyphenols. Formic acid was added to the mobile phase in order to

192 decrease the pH and improve the shape of the peaks and the chromatographic resolution, even
193 though it may inhibit the ionization of acidic compounds in the matrix (Chen, Lu, & Zhao, 2014).
194 Three gradients were tested on five different end-capped C18 columns (Hypersil Gold, HSST3,
195 BEH, Syncronis and Kinetex) and separation of astilbin and *epi*-DPA-G was achieved in all
196 cases. The efficiency of the gradients and columns were evaluated by comparing the validation
197 parameters (RSD, LOQ and LOD) for the injection of calibration solutions ranging from 0.02 to
198 10 mg/L. For each column, gradients **I** and **II** gave almost similar results, whereas gradient **III**
199 was the best for separating *epi*-DPA-G and astilbin (**Tables 2** and **3**). This is probably because
200 gradient **III** started with 90 % of 0.1 formic acid in water instead of 95 or 98 %, which
201 minimized the retention of the analytes and also reduced the clustering of peaks, especially when
202 analyzing the wine matrix. In addition, by extending the organic phase from 1 min to 7.5 min, a
203 better separation was achieved due to better interaction of the polar compounds with the
204 stationary phase, as illustrated by the better reproducibility of retention time and sensitivity.
205 The different tested C18 columns are end-capped. However, due to their manufacturing process
206 and geometry, their retention of analytes and their reproducibility and sensitivity are not the
207 same.
208 Hypersil Gold C18, used in our previous qualitative study (Crétin et al., 2019), is known to retain
209 compounds over a wide range of polarity. It has a proprietary derivatization system and has a
210 highly pure silica end cap that the manufacturers claim reduces peak tailing and improves
211 efficiency, particularly at very low pH (2-5). It is therefore used as stationary phase in LC-MS
212 applications (Fanigliulo et al., 2011). On the other hand, the T3 bonding of high silica strength
213 HSS uses a trifunctional C18 alkyl with a 1.8 µm bonded phase at a ligand density that promotes
214 the retention of small, water-soluble polar organic compounds and aqueous mobile phase
215 compatibility, so HSST3 could also be suitable for this study. The BEH C18 column incorporates

trifunctional ligand bonding chemistries on the 1.7 µm BEH particles based on new end-capping processes that ensure good peak shape for basic analytes (Gritti & Guiochon, 2013; New & Chan, 2008). Syncronis C18 has been engineered to provide good reproducibility thanks to its highly pure and high surface area silica, dense bonding and double endcapping that minimizes secondary interactions (« Column range delivers reproducibility », 2010). Indeed, good reproducibility was obtained when using this column (**Tables 2** and **3**). Finally, Kinetex C18 is a uniform porous silica layer grown around a spherical solid silica core. This combination of precise particle architecture provides dramatic leaps in performance and increases the rate of mass transfer by decreasing the effects of diffusion and reducing losses in efficiency (Gritti et al., 2017).

In this study, Hypersil Gold C18 was the most suitable column to quantify the targeted compounds, especially when using gradient **III**. An efficient and rapid separation with good resolution was obtained since *epi*-DPA-G and astilbin eluted at 1.4 and 3.6 min, respectively, which is important for routine analysis. The ionization parameters were optimized by automatic tune for astilbin and *epi*-DPA-G. For each sample analyzed, extracted ion chromatograms (XIC) were built in a 5 ppm window around the empirical formula of each compound. *Epi*-DPA-G with a composition of $C_{21}H_{32}O_{10}$ presented a HRMS spectrum with a quasi-molecular $[M\text{-}H]^-$ ion at *m/z* 443.19028, while astilbin with the empirical formula $C_{21}H_{22}O_{10}$ had a $[M\text{-}H]^-$ ion at *m/z* 449.10681.

The validation studies were performed in accordance with the regulatory guidelines stipulating that a method used for the quantitative measurement of analytes should be reliable and reproducible for the intended use (Pereira et al., 2018) (http://www.labcompliance.de/documents/FDA/FDA-Others/Laboratory/f-507-bioanalytical-4252fnl.pdf). Results summarized in ***section 3.2***. and in **Tables 2** and **3** demonstrate good

240 reproducibility for all the columns with the best value obtained with Hypersil, for which intra-
241 day RSD_{tr} was 0.20 % for *epi*-DPA-G and astilbin. To perform the quantification, other
242 validation parameters such as linearity, RSD_A, LOQ, LOD and recovery were also evaluated.
243

244 ### *3.2. Additional validation parameters*

245 #### *3.2.1. Linearity*

246 The parameters of the standard calibration curves obtained from the average concentration of *epi*-
247 DPA-G and astilbin at seven different levels, using three gradients and on five C18 columns are
248 presented in **Tables 2** and **3**. The resulting correlation coefficient (r^2) makes it possible to
249 estimate the linearity of the curve obtained. Depending on the columns and the gradients, r^2
250 values were obtained from 0.9837 to 0.9999 for *epi*-DPA-G and from 0.8542 and 0.9992 for
251 astilbin in the concentration range 0.02 - 10 mg/L. This range was chosen for the linearity study,
252 since it included the concentrations of *epi*-DPA-G and astilbin estimated in the tested red wines.
253 For *epi*-DPA-G, the calibration curves were satisfactorily linear, especially for Hypersil and
254 HSST3 with all gradients. For the three other columns, the best results were obtained with
255 gradients **I** and **II**. For astilbin, the correlation coefficients (r^2) were strongly affected by the
256 column and the best values were obtained with Hypersil ($r^2 \geq 0.9980$ for all gradients) and, to a
257 lesser extent, with Kinetex ($r^2 \geq 0.9927$).

258 #### *3.2.2. LOD and LOQ*

259 LOQ and LOD (**Tables 2** and **3)** were evaluated using a linearity approach. For both compounds,
260 the best sensitivity was obtained when using gradient **III** with Hypersil. In these conditions, LOQ
261 was 18 and 20 µg/L for *epi*-DPA-G and astilbin, respectively. Extracted ion chromatograms of

262 *epi*-DPA-G and astilbin at 10 µg/L (similar to that of LOD) are presented in the **supporting**
263 **information (Figure S-1)**.

264 ***3.2.3. Intra- and inter-day precision (RSD)***

265 RSD_A was evaluated for *epi*-DPA-G and astilbin in the different chromatographic conditions.
266 Good intra-day repeatabilities were obtained for all columns but with a preference for Hypersil,
267 for which RSD_A was 3.0% and 2.0% for *epi*-DPA-G and astilbin, respectively (**Tables 2** and **3**).
268 In these conditions, inter-day repeatabilities on retention times and peak areas for *epi*-DPA-G
269 and astilbin evaluated were lower than 3.5 % (n=3).

270 ***3.2.4. Recovery***

271 Based on the previous linearity, sensitivity and repeatability results, gradient **III** and Hypersil
272 columns were selected for the quantitative study. Recovery was evaluated for both compounds in
273 these conditions. Three known concentrations of *epi*-DPA-G and astilbin (100 µg/L; 500 µg/L
274 and 1 mg/L) were spiked in PO1999b, SES2001 and VPCR1992. The recovery values ranged
275 from 89 to 99 %, which meets the requirements of the guidelines (**Table 4**). Therefore, this
276 method is suitable for quantifying *epi*-DPA-G and astilbin in red wine.

277

278 ***3.3. Application of method for quantification of epi-DPA-G and astilbin in various French***
279 ***commercial red wines***

280 After validating the method by using gradient **III** and the Hypersil column, several vintages of French red
281 wines from four wine regions and 15 appellations were assayed (**Table 1**). The concentrations of *epi*-
282 DPA-G and astilbin quantified in wine were determined from the calibration curve of the purified
283 standards and by considering the dilution factor. *Epi*-DPA-G was detected at 1.40 min and astilbin at 3.62

284 min. Therefore, this demonstrates the selectivity of the method to identify and quantify *epi*-DPA-G and
285 astilbin in wine. However, additional peaks with the same mass and molecular formula were
286 present at 2.53, 3.45 and 3.96 min, suggesting the possible presence of astilbin isomers. These
287 additional peaks were almost present in the different vintages of the red wine tested and could be
288 separated by using gradient **III**. An example of an extracted ion chromatogram (XIC) of *epi*-
289 DPA-G and astilbin present in a PO1999b and obtained by using gradient **III** on Hypersil C18 is
290 illustrated in **Figure 1.**
291 As shown in the **supporting information (Table S-1)**, *epi*-DPA-G and astilbin were observed in all
292 wines, at concentrations varying strongly according to the origins and the vintages. *Epi*-DPA-G
293 concentrations ranged from 1.2 to 14.7 mg/L with a mean value of 7.3 mg/L. The lowest quantity
294 of *epi*-DPA-G was present in CL2013 and the highest quantity in CL1923. Astilbin
295 concentrations ranged from 0.5 mg/L (in MA1990) to 42.6 mg/L (in CL2015) with a mean value
296 of 8.1 mg/L. Box plots of CL showed a range of *epi*-DPA-G from 1.2 to 14.7 mg/L and a range
297 of astilbin from 8.5 to 42.8 mg/L **(Figure 2).** Therefore, *epi*-DPA-G and astilbin are highly
298 present in CL.
299 In this study, *epi*-DPA-G was quantified for the first time in wine. Moreover, astilbin
300 concentrations obtained were in the same range of those obtained in the literature (K. Trousdale
301 & L. Singleton, 1983; Landrault et al., 2002). On the other hand, the effect of vintage on astilbin
302 concentrations had never been described until now. The analysis of 16 vintages of the same
303 estate (Clos des Lambrays) revealed high concentrations of both compounds in one-century-old
304 wines, which suggests that they are not significantly degraded over time.
305
306 **Conclusion**

An LC-FTMS method has been developed to identify and quantify two sweet molecules present in wines: *epi*-DPA-G and astilbin. Five columns and three gradients were tested to optimize the conditions of analysis. The method is satisfactory in terms of sensitivity, linearity, repeatability and recovery and was applied successfully to quantify *epi*-DPA-G and astilbin in several commercial red wines. *Epi*-DPA-G was quantified in wine for the first time. Both compounds were present at concentrations ranging from a few mg/L to a few tens of mg/L. The presence of high amounts in one-century-old wines suggests the relative stability of both compounds over time. Therefore, this method can now be used to study the effect of grape varieties, origins and maturity on the presence of these sweet compounds. The development of this method brings a new tool that will be useful to investigate the influence of viticultural and enological parameters on the taste of wine. Finally, some astilbin isomers never identified until now in wine were detected in some samples. Future work will focus on the isolation, structural elucidation and sensory assessment of these compounds to determine their potential contribution to sweetness in dry wines.

Acknowledgements

The authors declare that there are no conflicts of interest.

References

Acunha, T., Simó, C., Ibáñez, C., Gallardo, A., & Cifuentes, A. (2016). Anionic metabolite profiling by capillary electrophoresis-mass spectrometry using a noncovalent polymeric coating. Orange juice and wine as case studies. *J. Chromatogr. A*, *1428*, 326-335.

Chen, S.-D., Lu, C.-J., & Zhao, R.-Z. (2014). Qualitative and quantitative analysis of Rhizoma Smilacis glabrae by ultra high performance liquid chromatography coupled with LTQ orbitrapXL hybrid mass spectrometry. *Molecules*, *19*(7), 10427-10439.

Column range delivers reproducibility. (2010). *Filtration + Separation*, *47*(6), 14.

Coste, A., Sousa, P., & Malfeito-Ferreira, M. (2018). Wine tasting based on emotional responses: An expedite approach to distinguish between warm and cool climate dry red wine styles. *Food Res. Int.*, *106*, 11-21.

Crétin, B. (2016). *Recherches sur les déterminants moléculaires contribuant à l'équilibre gustatif des vins secs*. École doctorale des sciences de la vie et de la santé-Spécialié oenologie, University of Bordeaux.

Crétin, B., Waffo-Teguo, P., Dubourdieu, D., & Marchal, A. (2019). Taste-guided isolation of sweet-tasting compounds from grape seeds, structural elucidation and identification in wines. *Food Chem.*, *272*, 388-395.

De Paepe, D., Servaes, K., Noten, B., De Loose, M., Van Droogenbroeck, B., & Voorspoels, S. (2013). An improved mass spectrometric method for identification and quantification of phenolic compounds in apple fruits. *Food Chem.*, *136*(2), 368-375.

De Revel, G., Darriet, P., Dubourdieu, D., Maujean, A., Glories, A., & Ribereau-Gayon, P. (2017). *Traité d'oenologie - Tome 2 Chimie du vin. Stabilisation et traitements*.

348 Del Refugio Ramos, M., Jerz, G., Villanueva, S., López-Dellamary, F., Waibel, R., &
349 Winterhalter, P. (2004). Two glucosylated abscisic acid derivates from avocado seeds
350 (Persea americana Mill. Lauraceae cv. Hass). *Phytochem.*, *65*(7), 955-962.
351 Esteves, V., Lima, S., Lima, D., & Duarte, A. (2004). Using capillary electrophoresis for the
352 determination of organic acids in Port wine. *Anal. Chim. Acta*, *513*(1), 163-167.
353 Fanigliulo, A., Cabooter, D., Bellazzi, G., Allieri, B., Rottigni, A., & Desmet, G. (2011). Kinetic
354 performance of reversed-phase C18 high-performance liquid chromatography columns
355 compared by means of the kinetic plot method in pharmaceutically relevant applications.
356 *J. Chromatogr. A*, *1218*(21), 3351-3359.
357 Francis, I. L., & Williamson, P. O. (2015). Application of consumer sensory science in wine
358 research. *Aust. J. Grape Wine Res.*, *21*(S1), 554-567.
359 Gritti, F., & Guiochon, G. (2013). Adsorption behaviors of neutral and ionizable compounds on
360 hybrid stationary phases in the absence (BEH-C18) and the presence (CSH-C18) of
361 immobile surface charges. *J. Chromatogr. A*, *1282*, 58-71.
362 Gritti, F., Leonardis, I., Shock, D., Stevenson, P., Shalliker, A., & Guiochon, G. (2017).
363 Performance of columns packed with the new shell particles, Kinetex-C18. *J.*
364 *Chromatogr. A*, *1217*(10), 1589-1603.
365 Haseeb, S., Alexander, B., Santi, R.L., Liprandi, A.S., Baranchuk, A., (2019). What's in wine? A
366 clinician's perspective, *Trends Cardiovas. Med. 29*, 97–106.
367 Hogenboom, A. C., van Leerdam, J. A., & de Voogt, P. (2009). Accurate mass screening and
368 identification of emerging contaminants in environmental samples by liquid
369 chromatography–hybrid linear ion trap Orbitrap mass spectrometry. *J. Chromatogr. A*,
370 *1216*(3), 510-519.

371 Huang, H.-S., & Liaw, E.-T. (2017). HPLC-DAD-MS method for Simultaneous quantitation of
372 flavonoids in Hypericum formosanum and antiglycation activity. *J. Pharm. Phytochem.*,
373 *6*(5), 854-858.
374 Hufnagel, J. C., & Hofmann, T. (2008). Orosensory-directed identification of astringent
375 mouthfeel and bitter-tasting compounds in red wine. *J. Agric. Food Chem.*, *56*(4),
376 1376-1386.
377 K. Trousdale, E., & L. Singleton, V. (1983). Astilbin engeletin in grapes and wine. *Phytochem.*,
378 *22*(2), 619-620.
379 L. Waterhouse, A., L. Sacks, G., & W. Jefferey, D. (2016). *Understanding Wine Chemistry*.
380 Landrault, N., Larronde, F., Delaunay, J.-C., Castagnino, C., Vercauteren, J., Merillon, J.-M., …
381 Teissedre, P.-L. (2002). Levels of stilbene oligomers and astilbin in french varietal wines
382 and in grapes during noble rot development. *J. Agric. Food Chem.*, *50*(7), 2046-2052.
383 Lorrain, B., Ky, I., Pechamat, L., & Teissedre, P.-L. (2013). Evolution of analysis of polyhenols
384 from grapes, wines, and extracts. *Molecules*, *18*(1), 1076-1100.
385 Loureiro, V., Brasil, R., & Malfeito-Ferreira, M. (2016). A new wine tasting approach based on
386 emotional responses to rapidly recognize classic european wine styles. *Beverages*, *2*(1), 6.
387 MadalenaSena-Esteves, M., Mota, M., & Malfeito-Ferreira, M. (2018). Patterns of sweetness
388 preference in red wine according to consumer characterisation. *Food Res. Int.*, *106*,
389 38-44.
390 Malec, P. A., Oteri, M., Inferrera, V., Cacciola, F., Mondello, L., & Kennedy, R. T. (2017).
391 Determination of amines and phenolic acids in wine with benzoyl chloride derivatization
392 and liquid chromatography–mass spectrometry. *J. Chromatogr. A*, *1523*, 248-256.

393 Marchal, A., Marullo, P., Moine, V., & Dubourdieu, D. (2011). Influence of yeast
394 macromolecules on sweetness in dry wines: role of the saccharomyces cerevisiae protein
395 Hsp12. *J. Agric. Food Chem.*, *59*(5), 2004-2010.
396 Marchal, A., Pons, A., Lavigne, V., & Dubourdieu, D. (2013). Contribution of oak wood ageing
397 to the sweet perception of dry wines. *Aust. J. Grape Wine Res.*, *19*(1), 11-19.
398 Marchal, A., Waffo-Teguo, P., Génin, E., Mérillon, J. M., & Dubourdieu, D. (2011).
399 Identification of new natural sweet compounds in wine using centrifugal partition
400 chromatography-gustatometry and Fourier transform mass spectrometry. *Anal. Chem.*, *83*,
401 9629-9637.
402 Markoski, M. M., Garavaglia, J., Oliveira, A., Olivaes, J., & Marcadenti, A. (2016). Molecular
403 properties of red wine compounds and cardiometabolic benefits. *Nutr. Metab. Insights*, *9*,
404 51-57.
405 New, L.-S., & Chan, E. C. Y. (2008). Evaluation of BEH C18, BEH HILIC, and HSS T3 (C18)
406 column chemistries for the UPLC-MS-MS analysis of glutathione, glutathione disulfide,
407 and ophthalmic acid in mouse liver and human plasma. *J. Chromatogr. Sci.*, *46*(3),
408 209-214.
409 Pereira, R. C., Alves Nonatoa, C. de F., Camilo, C. J., Melo Coutinho, H. D., Rodrigues, F. F. G.,
410 Xiao, J., & Martins da Costa, J. G. (2018). Development and validation of a rapid RP-
411 HPLC-DAD analysis method for the quantification of pilocarpine in Pilocarpus
412 microphyllus (Rutaceae). *Food Chem. Toxicol.*, *119*, 106-111.
413 Pinto, J., Oliveira, A. S., Lopes, P., Roseira, I., Cabral, M., Bastos, M. de L., & Guedes de Pinho,
414 P. (2019). Characterization of chemical compounds susceptible to be extracted from cork
415 by the wine using GC-MS and 1H NMR metabolomic approaches. *Food Chem.*, *271*,
416 639-649.

Ribereau-Gayon, P., Dubourdieu, D., Doneche, B., & Lonvaud, A. (2017). *Traité d'oenologie - Tome 1 - 7e édition- Microbiologie du vin. Vinifications*.

Thompson, M., Ellison, S. L. R., & Wood, R. (2002). Harmonized guidelines for single-laboratory validation of methods of analysis (IUPAC Technical Report). *Pure Appl. Chem.*, *74*(5), 835–855.

Figure 1: Extracted ion chromatogram and mass spectra of a) *epi*-DPA-G and b) astilbin present in a PO1999b.

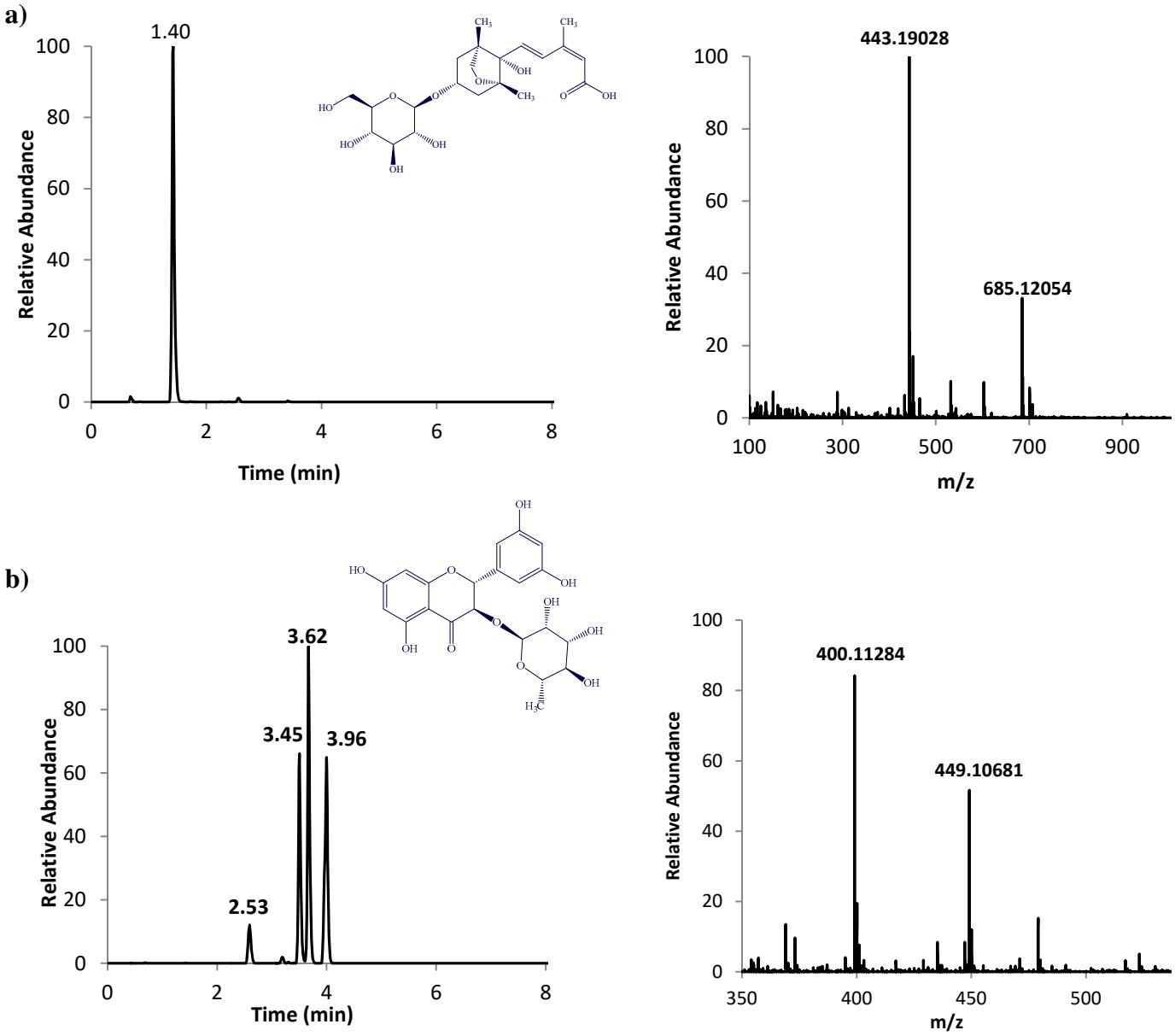

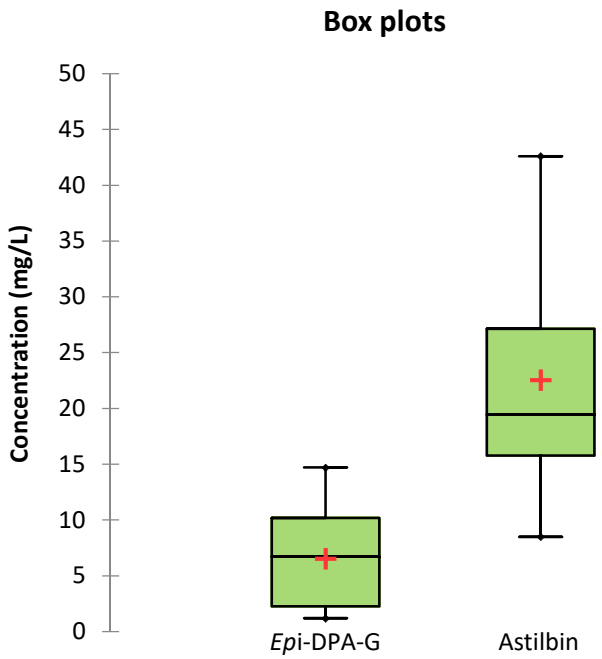

Figure 2: Box plots of *epi*-DPA-G and astilbin in several vintages of CL.

Table 1: Origin, vintage and grape varieties of the commercial wines used for quantification assays

Apellation	Vintage	Grape variety*	Region	
Pomerol	1981	M, CF, Ma	Bordeaux	**PO1981a**
Pomerol	1981	M, CF	Bordeaux	**PO1981b**
Pomerol	1981	M, CF	Bordeaux	**PO1981c**
Pomerol	1988	M, CF	Bordeaux	**PO1988**
Pomerol	1998	M, CF, CS	Bordeaux	**PO1998**
Pomerol	1999	M, CF	Bordeaux	**PO1999a**
Pomerol	1999	M, CF	Bordeaux	**PO1999b**
Pomerol	2007	M, CF	Bordeaux	**PO2007a**
Pomerol	2007	M	Bordeaux	**PO2007b**
Pomerol	2007	M, CF	Bordeaux	**PO2007c**
Pomerol	2008	M, CF	Bordeaux	**PO2008**
Saint-Julien	1998	CS, M, CF	Bordeaux	**SJ1998a**
Saint Julien	1998	CS, M, CF, PV	Bordeaux	**SJ1998b**
Saint Julien	1998	CS, M, CF, PV	Bordeaux	**SJ1998c**
Saint Julien	1999	CS, M, CF	Bordeaux	**SJ1999**
Saint Julien	2000	CS, M, CF	Bordeaux	**SJ2000**
Saint Julien	2002	CS, M, CF, PV	Bordeaux	**SJ2002a**
Saint Julien	2002	M, CS, CF	Bordeaux	**SJ2002b**
Saint Julien	2004	CS, M, CF	Bordeaux	**SJ2004**
Saint Julien	2007	CS, M	Bordeaux	**SJ2007a**
Saint Julien	2007	CS, M, CF, PV	Bordeaux	**SJ2007b**
Saint Julien	2008	CS, M, CF, PV	Bordeaux	**SJ2008a**
Saint Julien	2008	CS, M, CF	Bordeaux	**SJ2008b**
Saint Julien	2008	CS, M, CF, PV	Bordeaux	**SJ2008c**
Saint Emilion Grand cru	2003	M, CF	Bordeaux	**SE2003**
Saint Emilion Grand cru	2006	M, CF	Bordeaux	**SE2006**
Saint Emilion Grand Cru	2007	CF, M	Bordeaux	**SE2007**

Saint Emilion Grand cru	2013	M, CF	Bordeaux	**SE2013**
Saint-Emilion Grand Cru	2014	M, CF, CS	Bordeaux	**SE2014**
Margaux	1990	CS, M	Bordeaux	**MA1990**
Margaux	1997	CS, M	Bordeaux	**MA1007**
Margaux	2002	CS, M, CF, PV	Bordeaux	**MA2002a**
Margaux	2002	CS, M	Bordeaux	**MA2002b**
Pauillac	1999	CS, M, CF	Bordeaux	**PA1999**
Pauillac	2002	CS, M, CF	Bordeaux	**PA2002**
Pauillac	2005	CS, M, PV	Bordeaux	**PA2005**
Medoc	2004	M, CS, CF	Bordeaux	**ME2004**
Medoc	2009	M, CS, CF	Bordeaux	**ME2009**
Medoc	2014	M, CS, CF	Bordeaux	**ME2014**
Haut-Medoc	1983	M, CS, PV, CF	Bordeaux	**HM1983**
Haut-Medoc	1984	M, CS, PV, CF	Bordeaux	**HM1984**
Pessac-Léognan	1994	CS, M	Bordeaux	**PL1994**
Pessac-Léognan	2006	CS, M, PV	Bordeaux	**PL2006**
Pessac-Léognan	2008	CS, M, PV	Bordeaux	**PL2008**
Graves	2006	CS, M	Bordeaux	**GR2006**
Graves	2008	CS, M	Bordeaux	**GR2008**
Premières Côtes de Bordeaux	2007	M, PV, CS	Bordeaux	**PCB2007**
Premères Côtes de Bordeaux	2008	M, PV, CS	Bordeaux	**PCB2008**
Saint Estèphe	2001	M, CS, PV, CF	Bordeaux	**SES2001**
Clos des Lambrays	1918	PN	Bourgogne	**CL1918**
Clos des Lambrays	1919	PN	Bourgogne	**CL1919**
Clos des Lambrays	1923	PN	Bourgogne	**CL1923**
Clos des Lambrays	1934	PN	Bourgogne	**CL1934**
Clos des Lambrays	1937	PN	Bourgogne	**CL1937**
Clos des Lambrays	1946	PN	Bourgogne	**CL1946**
Clos des Lambrays	1949	PN	Bourgogne	**CL1949**
Clos des Lambrays	1950	PN	Bourgogne	**CL1950**
Clos des Lambrays	1967	PN	Bourgogne	**CL1967**

Clos des Lambrays	1972	PN	Bourgogne	**CL1972**
Clos des Lambrays	1997	PN	Bourgogne	**CL1997**
Clos des Lambrays	2003	PN	Bourgogne	**CL2003**
Clos des Lambrays	2005	PN	Bourgogne	**CL2005**
Clos des Lambrays	2013	PN	Bourgogne	**CL2013**
Clos des Lambrays	2015	PN	Bourgogne	**CL2015**
Clos des Lambrays	2017	PN	Bourgogne	**CL2017**
Vin de Pays des Collines Rhodaniennes	1992	S	Rhône Valley	**VPCR1992**
Crozes Hermitage	2014	S	Rhône Valley	**CH2014**
Vin de Pays d'Oc	2001	M	Languedoc Roussillon	**VPO2001**

* Cabernet Franc : CF ; Cabernet Sauvignon : CS ; Malbec : Ma ; M : Merlot ; Petit Verdot : PV ; Pinot Noir : PN ; Syrah : S

Table 2: Evaluation of validation parameters of *epi*-DPA-G on five columns using three different gradients

Column	Gradient	LOQ (µg/L)	LOD (µg/L)	RSD_{tr} (%)	RSD_A (%)	Linearity	
Hypersil	**I**	1930	643	0.6	3.5	r^2=0.9992	a= $4x10^6$ b=- $1.9x10^5$
	II	150	50	0.5	3.0	r^2= 0.9992	a= $8x10^6$ b=- $1.9x10^5$
	III	18	6	0.2	3.0	r^2= 0.9998	a=$4x10^6$ b=$-9.9x10^4$
HSST3	**I**	1039	346	1.1	3.4	r^2= 0.9997	a=$3x10^6$ b=$4.2x10^4$
	II	54	18	0.5	12	r^2=0.9973	a=$2x10^6$ b=$2.7x10^4$
	III	102	33	0.5	3.0	r^2=0.9960	a=$4x10^6$ b=2.10^6
BEH	**I**	280	93	1.4	4.6	r^2=0.9995	a=$3x10^6$ b=$-3.3x10^5$
	II	39	13	1.3	3.0	r^2=0.9941	a=$2x10^6$ b=$-2.9x10^5$
	III	65	21	0.5	7.0	r^2=0.9837	a=$3x10^6$ b=$-1.9x10^5$
Syncronis	**I**	1940	647	1.4	5.7	r^2=0.9999	a=$3x10^6$ b=$-4.3x10^5$
	II	247	83	0.5	3.4	r^2=0.9950	a=$1x10^6$ b=$-2.9x10^5$
	III	585	195	0.4	6.0	r^2=0.9898	a=$2x10^6$ b=$3.8x10^5$
Kinetex	**I**	2500	833	1.9	5.0	r^2=0.9992	a=$2x10^6$ b=$-9.7x10^4$
	II	240	80	0.4	8.0	r^2=0.9981	a=$2x10^6$ b=$-2.2x10^5$
	III	95	31	1.2	4.3	r^2=0.9844	a=$3x10^6$ b=$-1x10^6$

Table 3: Evaluation of validation parameters of astilbin on five different columns using three different gradients

Column	Gradient	LOQ (µg/L)	LOD (µg/L)	RSD_{tr} (%)	RSD_A (%)	Linearity	
Hypersil	I	45	15	0.2	7.0	r^2=0.9992	a=2.9x10^5 b=-1.1x10^5
	II	29	10	0.1	5.0	r^2=0.9992	a=6.1x10^5 b=-8.2x10^4
	III	20	7	0.1	2.0	r^2=0.9980	a=6.8x10^5 b=-1.1x10^5
HSST3	I	29	10	0.3	8.0	r^2=0.9945	a=2.8x10^5 b=-2.3x10^3
	II	27	9	0.2	12.0	r^2=0.9944	a=3.1x10^5 b=9.4x10^3
	III	23	8	0.6	6.0	r^2=0.9933	a=7.6x10^5 b=1.1x10^5
BEH	I	124	40	0.2	10.9	r^2=0.8542	a=1.1x10^5 b=-1.7x10^5
	II	100	34	0.3	8.1	r^2=0.8886	a=9.1x10^4 b=-4.9x10^4
	III	320	114	0.9	5.2	r^2=0.9205	a=5.1x10^5 b=-4.2x10^5
Syncronis	I	124	38	0.2	10.1	r^2=0.9542	a=1.2x10^5 b=-1.4x10^5
	II	340	120	0.4	19.0	r^2=0.9385	a=5.5x10^4 b=-3.7x10^4
	III	198	66	0.8	4.0	r^2=0.9898	a=1.6x10^5 b=6.9x10^4
Kinetex	I	120	40	0.2	15.0	r^2=0.9927	a=1.8x10^5 b=-2.5x10^3
	II	240	80	0.2	4.0	r^2=0.9982	a=2.2x10^5 b=-4.5x10^4
	III	203	67	3.0	9.0	r^2=0.9973	a=4.4x10^5 b=-9.6x10^4

Table 4: Recovery (%) of *epi*-DPA-G and astilbin in PO1999b, SES2001 and VPCR1992

Recovery (%) / Spiked concentrations (µg/L)	PO1999b		SES2001		VPCR1992	
	***Epi*-DPA-G**	**Astilbin**	***Epi*-DPA-G**	**Astilbin**	***Epi*-DPA-G**	**Astilbin**
100	94	89	91	89	95	93
500	89	96	92	95	92	89
1000	95	90	97	91	99	90